Constitutive Activation of Opsin by Mutation of Methionine 257 on Transmembrane Helix 6†

May Han,‡,§ Steven O. Smith,|| and Thomas P. Sakmar*,‡,⊥

Laboratory of Molecular Biology and Biochemistry, Howard Hughes Medical Institute, Rockefeller University, New York, New York 10021, and Department of Molecular Biophysics and Biochemistry, Yale University, New Haven, Connecticut 06520

Received January 20, 1998; Revised Manuscript Received April 6, 1998

ABSTRACT: Rhodopsin is a member of the large family of G protein-coupled receptors (GPCR's). Constitutive activity of GPCR's, defined as ligand-independent signaling, has been recognized as an important feature of receptor function and has also been implicated in the molecular pathophysiology of a number of human diseases. Rhodopsin has evolved a unique mechanism to minimize receptor basal activity. The chromophore 11-*cis*-retinal, which acts as an inverse agonist in rhodopsin, is covalently bound to the receptor to ensure extremely low receptor signaling in the dark. In this study, we replaced Met^{257} in TM helix 6 of opsin with each of the remaining 19 amino acids. Only mutant opsin M257R failed to be expressed in COS-cell membranes. Each of the remaining 18 mutant opsins, with the exception of M257L, was significantly constitutively active. Two mutants in particular, M257Y and M257N, displayed very high levels of constitutive activity. In addition, the double-site mutants with substitutions of both Met^{257} and Glu^{113} in TM helix 3 tended to be much more constitutively active than the sums of the activities of the individual single-site mutants. Based on existing structural models of rhodopsin, we conclude that Met^{257} may form an important and specific interhelical interaction with a highly conserved NPXXY motif in TM helix 7, which stabilizes the inactive receptor conformation by preventing TM helix 6 movement in the absence of *all-trans*-retinal. Furthermore, we are able to show that the pharmacological properties of the large number (∼50) of mutant opsins that we have characterized to date support the two-state model of GPCR function. These results suggest that rhodopsin and other GPCR's share a common mechanism of receptor activation that involves specific changes in helix−helix interactions.

G protein-coupled receptors (GPCR's)[1] comprise a large family of cell surface receptors that transduce information from the extracellular environment across the membrane to the interior of the cell. Constitutive activity of GPCR's, defined as ligand-independent signaling, has been recognized as an important feature of these receptors since it was first reported to occur in mutant α_{1B}-adrenergic receptors (*1*). Certain receptors also have intrinsically high levels of basal activity, which may be important for their physiological function (*2*, *3*). Increases in signaling in the absence of ligand can also result from overexpression of either the receptor (*4*) or the G protein (*5*). Conversely, rhodopsin (Rho), the visual rod cell photoreceptor responsible for dim-light vision, has evolved a unique mechanism to minimize receptor basal activity. The chromophore 11-*cis*-retinal, which acts as an inverse agonist in Rho, is covalently bound to the receptor to ensure extremely low receptor signaling in the dark.

Mutations responsible for certain human diseases have been found to cause constitutive activation of GPCR's. The mutant receptors responsible for these diseases are characterized by gain of function in vivo and in vitro. The diseases include: familial male precocious puberty caused by constitutive activity of the luteinizing hormone receptor (*6*−*8*); hyperfunctioning thyroid adenoma caused by constitutive activity of the thyrotropin receptor (*9*−*11*); hypocalcemia caused by constitutive activity of the Ca^{2+}-sensing receptor (*12*); Jansen-type metaphyseal chondrodysplasia caused by constitutive activity of the parathyroid hormone-related peptide receptor (*13*). This partial list is likely to grow over time. In addition, a virus encoded GPCR, homologous to the human interleukin-8 receptor, is found to stimulate cellular proliferation by constitutively activating the phosphoinositide−inositol triphosphate−protein kinase C pathway, qualifying the receptor gene as a candidate viral oncogene (*14*).

Rho mutants that are constitutively active in vitro have also been found in retinal diseases (*15*). Congenital night blindness is caused by the Rho mutations G90D or A292E (*16*, *17*), and forms of autosomal dominant retinitis pigmen-

† Support was provided by the Allene Reuss Memorial Trust to T.P.S., who is an Associate Investigator of the Howard Hughes Medical Institute. M.H. is a Charles H. Revson Fellow in Biomedical Research. S.O.S. was supported in part by NIH Grant GM 41412.

* Address correspondence to this author. E-mail: sakmar@rockvax.rockefeller.edu.

‡ Rockefeller University.

§ Present address: Howard Hughes Medical Institute, Department of Molecular Biophysics and Biochemistry, Yale University, New Haven, CT 06520.

|| Yale University.

⊥ Howard Hughes Medical Institute.

[1] Abbreviations: ATR, *all-trans*-retinal; DM, *n*-dodecyl β-D-maltoside; GPCR's, G protein-coupled receptors; G_t, transducin; Rho, rhodopsin; ROS, rod outer segment; TM, transmembrane.

S0006-2960(98)00147-0 CCC: $15.00
Published on Web 05/12/1998

tosa are caused by the mutations K296E or K296M (*18*−*21*). However, the pathophysiology of these visual disorders may be different from other diseases listed above in that elevated basal receptor activation in vivo has not been documented. One of the differences between Rho and other GPCR's is that the inverse agonist 11-*cis*-retinal, which is able to suppress the constitutive activity of the mutant opsins G90D (*22*) and A292E (*16*), is present in cells containing the mutant receptors. The G90D and A292E mutant receptors exist, at least in part, in the inactive ligand-bound form rather than the constitutively active apo-receptor form. Interestingly, patients carrying G90D mutation were shown to have an elevated absolute threshold for visual perception (*17*). FTIR spectroscopy of expressed mutant pigment G90D also suggested a possible increased energy barrier to light-dependent receptor activation (*23*).

Rho mutants K296E and K296M, however, do not bind 11-*cis*-retinal due to the lack of the lysine for Schiff base attachment (*20*, *21*). Therefore, significant amounts of these mutant opsin apo-receptors may be present to activate the retinal G protein, transducin (G_t), independently of either light or ligand. The visual system is also equipped with an extremely efficient turn-off pathway, which is triggered even before the activation process reaches peak potential (*24*). In transgenic mice expressing K296E, the mutant opsin was found to be constitutively phosphorylated and to bind arrestin, which prevents constitutive G_t activation (*25*). Therefore, constitutively active Rho mutants may not necessarily manifest a gain-of-function phenotype in vivo.

Most, but not all, of the constitutively active mutants in GPCR's other than Rho are located in TM helix 6 and in the cytoplasmic loop connecting TM helices 5 and 6 (*10*, *26*−*28*). The sites in GPCR's where activating mutations have been reported are highlighted in Figure 1 at positions corresponding to those in bovine Rho. In contrast, most activating mutations of Rho have been shown to disrupt a salt bridge between Glu^{113} in TM helix 3 and Lys^{296} in TM helix 7 (*15*). This salt bridge is not conserved in GPCR's in general. We recently reported two additional constitutively active Rho mutants, M257A and F261V (*29*). The mechanism of activation in these mutant opsins was apparently not related to breaking the Glu^{113}−Lys^{296} salt bridge (*29*). Both Met^{257} and Phe^{261} are located in TM helix 6 in Rho, in the same region where activating mutations in many other GPCR's have been identified (Figure 1).

In this study, we replace Met^{257} in opsin with each of the remaining 19 amino acids. Each of the 18 mutant opsins that were expressed in COS-cell membranes, with the exception of M257L, was significantly constitutively active. In addition, the combination of the Met^{257} mutation with activating mutations of residues Glu^{113} or Glu^{134} in TM helix 3 produced double mutants with synergistic levels of activity. The double-site mutants tended to be much more active than the sums of the activities of the individual single-site mutants. These findings are reconciled with existing structural models of Rho. We conclude that Met^{257} may form an important and specific interhelical interaction that stabilizes the inactive receptor conformation by preventing TM helix 6 movement in the absence of *all-trans*-retinal. This stabilizing interaction may occur between Met^{257} and the NPXXY motif in TM helix 7, which is highly conserved in GPCR's. Furthermore, we are able to show that the pharmacological characteristics

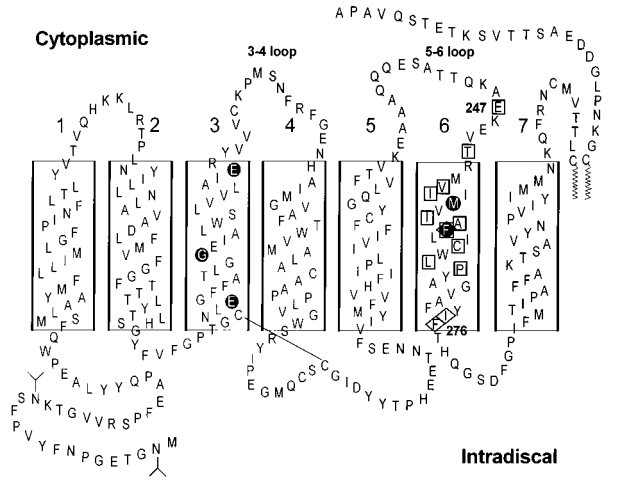

FIGURE 1: Schematic representation of bovine Rho secondary structure. The seven transmembrane α-helical segments are boxed and numbered. The N-terminus and intradiscal (extracellular) surface of the receptor are toward the bottom and the C-terminus and cytoplasmic surface are toward the top of the figure. Amino acid residues highlighted with black circles were studied in this report: Glu^{113}, Gly^{121}, Glu^{134}, Met^{257}, and Phe^{261}. Amino acid residues indicated by squares correspond to sites where mutation of the residue at the equivalent position in another GPCR caused constitutive activity: Glu^{247} (*9*, *10*), Thr^{251} (*9*, *10*, *39*, *64*), Val^{254} (*65*), Ile^{255} (*66*), Ile^{259} (*10*), Ala^{260} (*10*), Phe^{261} (*6*, *8*, *10*), Cys^{264} (*28*), Leu^{266} (*66*), and Pro^{267} (*67*). Amino acid residues indicated by diamonds correspond to sites where replacement of the residue at the equivalent position in another GPCR by proline abolished ligand binding and/or G protein signaling: Phe^{261} (*8*), Ile^{275} (*60*), and Phe^{276} (*68*). Note that Phe^{261} is found in all of the categories listed above.

of the large number (∼50) of mutant opsins that we have characterized to date support the two-state model of GPCR function (*30*, *31*). In summary, these results suggest that Rho and other GPCR's share a common mechanism of receptor activation that involves specific changes in helix−helix interactions.

EXPERIMENTAL PROCEDURES

Construction of 19 Mutant Opsin Genes with Replacements of Met^{257}. Site-directed mutagenesis was achieved using restriction fragment replacement (*32*) in a synthetic gene of Rho (*33*) cloned into an eukaryotic expression vector (*34*). The first set of Met^{257} mutants was constructed substituting a 103 base pair *Mlu*I−*Apa*I restriction fragment with a synthetic duplex containing NNC at codon 257 and a silent mutation at codon 267 to remove a *Nde*I site for the purpose of screening. The codon NNC codes for 16 different amino acids. The nucleotide sequences of multiple independent clones were determined using the chain termination method (United States Biochemical). Thirteen of the expected 16 codons were identified by sequencing 41 recombinant transformants. The three mutants not found in the first screen (M257I, M257V, and M257Y) and the mutant M257W were constructed using two additional synthetic duplexes, one containing codon KKG coding for M257W and M257V, and the other containing codon WWC coding for M257I and M257Y. The three Met^{257} mutants not encoded by the NNC codon (M257E, M257K, and M257Q) were constructed using the *Mlu*I−*Apa*I restriction fragment containing VAG at codon 257. These 3 mutants were identified by sequencing

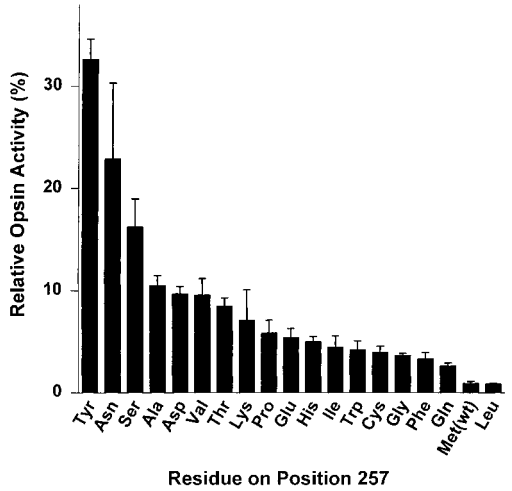

FIGURE 2: Constitutive activities of 18 individual opsin mutants with substitutions of Met^{257}. Each of 18 opsin mutants was assayed in COS-cell membranes for the ability to activate G_t. No chromophore was added to the membranes. M257L displayed the same basal level of activity as wild-type opsin. Other replacement mutations resulted in mutant opsins with significant constitutive activity. Mutant M257Y displayed activity greater than 30% of the value measured in light after the addition of 11-*cis*-retinal. Numerical values are presented in Table 1. Mutant M257R failed to be expressed at detectable levels in the COS-cell membranes.

10 recombinant transformants. The identity of each of the 19 mutant opsin genes was confirmed a second time by sequencing.

Expression and Characterization of Met^{257} Mutants. Expression, purification, spectroscopic characterization, and biochemical assay procedures were carried out as previously described (*35*).

RESULTS

Constitutive Activity of Mutant Opsins with Substitution of Met^{257}. Membranes were prepared from transiently transfected COS cells expressing each of the mutant opsins. No retinal chromophore was added to the membranes. The membrane samples were assayed for the ability to catalyze GTPγS uptake by purified ROS G_t. Mutant opsin M257R was not studied since it was not found at detectable levels in membrane preparations due to poor expression. A large number of other opsin mutants with substitutions of arginine for amino acids in the membrane-embedded domain of the receptor have also failed to be expressed at detectable levels (*36*). The activities of 18 Met^{257} mutant opsins and the basal activity of wild-type opsin are presented in Figure 2. The opsins in Figure 2 are arranged in order of decreasing constitutive activity. Numerical values are presented for each of the opsins in Table 1. The values are given as a percentage of the activity of the same membrane preparation assayed in parallel in light after regeneration with 11-*cis*-retinal. This method of normalization allows a direct comparison of constitutive activity relative to the maximal light-induced activity for different opsins (*29*, *35*). For example, the activity of wild-type opsin in membranes is 0.9% of the activity of wild-type opsin regenerated with 11-*cis*-retinal and measured under illumination, and M257Y exhibits an opsin activity that is 32.6% of its light activity. Seventeen of the Met^{257} mutant opsins display significant constitutive activity. The levels of activity range from a low of 2.6% for M257Q to a high of 32.6% for M257Y. Only mutant opsin M257L failed to display constitutive activity (0.8% versus 0.9% for wild-type opsin). Leucine is the most conservative substitution for methionine in terms of size and hydrophobicity. We considered possible quantitative correlations between the physicochemical properties of the amino acid side chain at position 257 and the level of constitutive activity of the mutant opsin. There is no readily discernible correlation between the level of constitutive activity and either the hydrophobicity scale (*37*) or the volume (*38*) of the side chain at position 257 when all the data are considered. A moderate correlation with size (correlation coefficient 0.67) can be derived when some of the mutants are not considered (i.e., M257Y, M257N, M257W, and M257G). It is interesting to note that mutants M257Y and M257N display the highest levels of opsin activity among those tested.

Table 1: G_t Activation by Opsin Met^{257} Mutants in COS-Cell Membranes[a]

mutant[b]	opsin[c] (%)	11-*cis*-retinal/dark[c] (%)	*all-trans*-retinal[c] (%)	11-*cis*-retinal/light[d] (%)
wild-type	0.9 ± 0.2 (5)	0.8 ± 0.3 (5)	14 ± 5 (4)	100
M257A	10.5 ± 1.0[e]	2.9 ± 1.0	112 ± 16[e]	102 ± 3[e]
M257C	3.9 ± 0.6	1.0 ± 0.1	73 ± 10	110 ± 26
M257D	9.7 ± 0.7	1.8 ± 0.2	80 ± 3	60 ± 9
M257E	6.4 ± 0.9	0.8 ± 0.4	86 ± 2	90 ± 6
M257F	3.3 ± 0.7	3.1 ± 1.8	67 ± 3	113 ± 6
M257G	3.6 ± 0.2	1.9 ± 0.6	66 ± 8	72 ± 7
M257H	5.0 ± 0.5	1.4 ± 0.4	80 ± 9	85 ± 4
M257I	4.4 ± 1.1	1.0 ± 0.2	71 ± 20	109 ± 5
M257K	7.1 ± 3.0	1.4 ± 0.6	91 ± 12	96 ± 8
M257L	0.8 ± 0.1	0.9 ± 0.0	17 ± 5	112 ± 14
M257N	22.9 ± 7.4	0.8 ± 0.4	93 ± 10	72 ± 9
M257P	5.8 ± 1.3	2.7 ± 0.6	47 ± 14	14 ± 1
M257Q	2.6 ± 0.3	1.3 ± 0.1	81 ± 3	94 ± 2
M257S	16.2 ± 2.7	4.2 ± 1.6	99 ± 16	87 ± 9
M257T	8.5 ± 0.8	3.8 ± 1.6	62 ± 5	98 ± 13
M257V	9.6 ± 1.6	2.1 ± 0.7	83 ± 13	81 ± 6
M257W	4.2 ± 0.9	1.7 ± 0.5	39 ± 11	69 ± 6
M257Y	32.6 ± 2.0	2.2 ± 1.2	98 ± 6	101 ± 3

[a] Values indicate the ability of opsin alone, opsin with 11-*cis*-retinal in the dark, opsin with *all-trans*-retinal in the dark, and opsin with 11-*cis*-retinal in the light to activate G_t. Values are given as mean ± SE, $n = 3$ unless otherwise specified. [b] Mutant opsin M257R was not detected in membrane preparations due to low expression level. [c] Opsin, 11-*cis*-retinal/dark, and *all-trans*-retinal activities are normalized to the 11-*cis*-retinal/light activity of the corresponding mutant measured in parallel. [d] Light activities in the presence of 11-*cis*-retinal are normalized to the light activity of wild-type opsin measured in parallel. [e] Values from Han et al. (*29*).

In the presence of 11-*cis*-retinal in the dark, the constitutively active Met^{257} mutant opsins, with the exception of M257F, exhibit lower activity than when measured without added chromophore. The 11-*cis*-retinal dark activity of M257F is equal to that of its opsin activity. As previously shown for mutant opsin E113Q (*21*), 11-*cis*-retinal can suppress basal opsin activity. It functions as an inverse agonist in Met^{257} mutant opsins with constitutive activity.

Activity of Mutant Opsins with Substitution of Met^{257} after Incubation with 11-cis-Retinal followed by Illumination. Membranes were prepared from COS cells expressing each of the mutant opsins. The 11-*cis*-retinal chromophore was added to the membrane preparations in the dark. The regenerated membranes were then assayed for the ability to catalyze GTPγS uptake by G_t under continuous illumination.

Twelve of the Met^{257} mutant opsins (M257A, M257C, M257E, M257F, M257H, M257I, M257K, M257L, M257Q, M257S, M257T, and M257Y) display essentially the same activity as Rho. Five of the mutant opsins (M257D, M257G, M257N, M257V, and M257W) display moderately reduced light activity (60−81%) relative to that of Rho. Only mutant opsin M257P is significantly impaired in its ability to activate G_t upon illumination. The M257P mutation may cause a kink in the α-helical secondary structure that disrupts normal helix−helix interactions necessary for G_t activation. Together these results imply that the methionine residue at position 257 is not specifically required for 11-*cis*-retinal binding nor G_t activation in response to light.

Activity of Mutant Opsins with Substitution of Met^{257} after Incubation with all-trans-Retinal. In these experiments, the chromophore *all-trans*-retinal was added to membrane preparations from COS cells expressing each of the mutant opsins. The membranes were then assayed for the ability to catalyze GTPγS uptake by G_t in the dark. The activities were normalized to the activities of the same membrane samples incubated with 11-*cis*-retinal in the dark and then illuminated as described above. The result is defined as *all-trans*-retinal activity (Table 1). For all of the opsins tested, the addition of *all-trans*-retinal increases its ability to activate G_t. It was noted previously that mutant opsins with high constitutive activity might also bind *all-trans*-retinal with higher affinity (*29*). The possible relationship between the level of basal or constitutive opsin activity and the ability of *all-trans*-retinal to act as an agonist ligand was explored. In Figure 3, relative *all-trans*-retinal activity is plotted as a function of opsin activity for each of the 19 opsins tested. In the case of wild-type opsin and mutant M257L opsin, the *all-trans*-retinal binding only results in a fraction of the activity observed after 11-*cis*-retinal binding followed by illumination. As presented in Figure 2 and Table 1, neither of these two opsins showed significant constitutive or basal activity. Each of the other Met^{257} mutant opsins, all of which are constitutively active, displays *all-trans*-retinal activity that is significantly higher than its respective constitutive activity. The *all-trans*-retinal activities for these 17 mutants range from 39% for M257W to 112% for M257A (Table 1). Relative *all-trans*-retinal activity increases rapidly at relatively low levels of constitutive activity and reaches a plateau of full activation when constitutive activity is above 10%. This relationship can be interpreted further in the context of the two-state model of GPCR function by plotting the ideal case predicted by the model as a smooth line in Figure 3 (see Discussion).

Spectral Properties of Purified Mutant Pigments with Substitution of Met^{257}. The Met^{257} mutant pigments were also purified in DM detergent solution. The UV−visible absorption spectra of these mutant pigments were measured, and parameters such as the λ_{max}, extinction coefficient (ϵ), and relative spectral ratio were derived (Table 2). Each of the Met^{257} mutant pigments displays essentially the same λ_{max} as that of Rho (500 nm). Only the λ_{max} of mutant pigment M257W (497 nm) varies slightly from the wild-type value. These results imply that the residue at position 257 does not participate in spectral tuning and is not likely to interact directly with the chromophore in the receptor ground state. This suggests that the effects of Met^{257} mutation that influence G_t binding do not perturb the retinal-binding pocket.

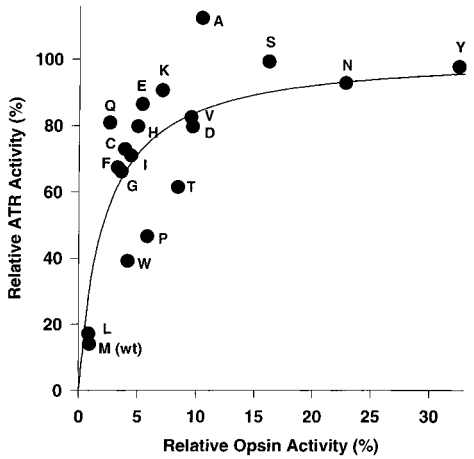

FIGURE 3: Activities of opsin Met^{257} mutants plotted according to the two-state model of GPCR activation (*30*). Each of the opsin mutants was assayed in COS-cell membranes for the ability to activate G_t. The level of activity in the presence of ATR is plotted as a function of the activity when no chromophore was added to the membranes. Each mutant is designated by the single-letter code of the amino acid substituted for Met^{257}. Numerical values are presented in Table 1. The relationship between opsin activity and ATR activity can be described by the two-state model. The two-state model predicts that the maximal fraction of receptor in the active form (f_{R^*}) is related to the equilibrium constant L (L = [R]/[R*], where [R] and [R*] are the concentrations of apo-receptor in the inactive and the active states, respectively) by the formula $f_{R^*} = 1/(1 + LK_{A^*}/K_A)$, where K_{A^*} and K_A are the equilibrium constants of receptor binding to ligand A in its active and inactive states (K_{A^*} = [R*][A]/[AR*], K_A = [R][A]/[AR]). In our system, L is related to the level of opsin activity for each mutant by the formula: L = 1/(opsin activity) − 1. ATR activities represent the maximal receptor activity under the experimental assay conditions since the opsin is fully saturated with agonist ligand at the concentration of ATR used to measure ATR activity (*35*). Therefore, the two-state model defines the following relationship between ATR activity and opsin activity: ATR activity = (opsin activity)/[(1 − k)(opsin activity) + k], where $k = K_{A^*}/K_A$. The curve represents the best fit of this equation to the experimental data points where k is assumed to remain constant for each mutant. The opsin mutants closely follow the curve predicted by the two-state model, with a k of 0.027 and a standard error of 16%.

The spectral ratio of a pigment (A_{280}/A at λ_{max}) reflects its ability to bind 11-*cis*-retinal and to remain stable during the purification procedure. Given ϵ, the spectral ratio of a mutant pigment can be normalized to that of Rho. The higher the relative spectral ratio, the more free opsin is copurified with a pigment. While the majority of the Met^{257} mutant pigments exhibit relative spectral ratios equal to or smaller than 1.20, several mutants display higher relative spectral ratios (Table 2). These mutants either contain a polar side chain at position 257 [M257D (1.28), M257N (1.33), and M257T (1.23)] or contain a side chain with extreme properties among the 20 amino acids [M257G (1.42), M257P (1.39), and M257W (1.66)]. Even through Met^{257} does not interact directly with the chromophore, it is not surprising that drastic substitutions would cause a decrease in the ability of the mutant to bind chromophore and/or in the stability of the resulting pigment.

Activation of G_t by Purified Met^{257} Mutant Pigments. The ability of the purified Met^{257} mutant pigments to activate G_t upon illumination was also measured and normalized to that of Rho assayed under the same conditions. A plot of

Table 2: Properties of Met^{257} Mutant Pigments Purified in Dodecyl Maltoside[a]

pigment[b]	λ_{max} (nm)	ϵ[c] ($\times 10^3$ M^{-1} cm^{-1})	relative spectral ratio[d]	G_t activation (%)[e]
Rho	500	42.7	1	100
M257A[f]	501 ± 0.2 (4)	40.2 ± 0.2 (2)	1.09 ± 0.03 (2)	52 ± 2
M257C	500 ± 0.3	41.3 ± 0.8 (2)	1.01 ± 0.02	87 ± 8
M257D	499 ± 1	36.8 ± 2.2 (2)	1.28 ± 0.05	55 ± 5
M257E	500 ± 0.3	43.3 ± 2.6 (2)	1.17 ± 0.06	58 ± 6
M257F	500 ± 0.3	41.7 ± 0.7 (2)	0.92 ± 0.08	86 ± 6
M257G	499 ± 0.6	43.6 (1)	1.42 ± 0.02	51 ± 2
M257H	500 ± 0.3	43.8 ± 3.3 (2)	1.07 ± 0.09	55 ± 6
M257I	500 ± 0.3	41.3 ± 0.03 (2)	1.08 ± 0.08 (2)	74 ± 6
M257K	499 ± 0.7	39.4 ± 2.3 (2)	1.19 ± 0.21	58 ± 6
M257L	500 ± 0.0	41.2 ± 0.02 (2)	0.97 ± 0.05 (4)	64 ± 2
M257N	499 ± 0.9	39.9 ± 2.9 (2)	1.33 ± 0.03	56 ± 3
M257P	498 ± 0.7	42.1 ± 1.1	1.39 ± 0.10 (4)	4.8 ± 0.6
M257Q	500 ± 0.3	42.0 ± 1.2 (2)	0.99 ± 0.04 (2)	82 ± 7
M257S	500 ± 0.0	42.6 ± 0.3	1.06 ± 0.10	67 ± 5
M257T	500 ± 0.3	42.7 ± 1.6	1.23 ± 0.09	62 ± 5
M257V	500 ± 0.0	41.4 ± 1.1	1.13 ± 0.08	55 ± 3
M257W	497 ± 2.4	43.9 ± 2.1	1.66 ± 0.08	60 ± 2
M257Y	500 ± 0.3	44.0 ± 1.1	1.03 ± 0.14 (2)	92 ± 10

[a] The data values are given as mean ± SE, $n = 3$ unless otherwise specified. [b] Mutant pigment M257R could not be purified due to low expression. [c] Molar extinction coefficient (ϵ) was determined as described (*35*). [d] Relative spectral ratio is A_{280}/A_{max} of a given pigment relative to that of Rho prepared in parallel. The A_{max} values of the mutant pigments are corrected for differences in ϵ. A_{280} and A_{max} are absorbance values of a given pigment at 280 nm and its visible λ_{max}, respectively. [e] G_t activation of a pigment under illumination is normalized to that of Rho measured in parallel. The pigment concentrations were determined by the absorption at λ_{max} and ϵ. [f] Data values for mutant pigment M257A are from Han et al. (*29*).

pigment-catalyzed GTPγS uptake by G_t as a function of time was used to determine the specific activity of each mutant (*35*). The numerical value for G_t activation for each of the mutant pigments relative to that of Rho is given in Table 2. As was observed in COS-cell membranes, mutant M257P exhibits low (4.8%) relative G_t activation in detergent compared to the other Met^{257} mutants. All of the other Met^{257} mutants display moderate G_t activation of between 51% and 92%. It is interesting to note that relative light activities were always higher in COS-cell membranes than in detergent for a given mutant. Both sets of activity data (i.e., membranes and detergent-purified pigments) were normalized to the values obtained for Rho prepared and measured in parallel (Tables 1 and 2). Light activities measured in COS-cell membranes are not corrected for effects of the mutation on expression levels. However, it is our experience that most mutations result in either no change or a decrease in opsin expression. This effect would cause an underestimation of the relative light activity measured in membranes. Therefore, the differences in light-induced activity observed in DM relative to that in COS-cell membranes may be understated in this study.

Synergistic Effects of Two Mutations in Conferring High Levels of Constitutive Activity. We previously reported that individual activating mutations in TM helices 3 and 6 sometimes behave synergistically (*29*). A double-site mutant opsin could have constitutive activity that was higher than the sum of the respective two individual single-site mutant opsins. In this study, we systematically constructed a panel of double-site mutants to explore the possibility of obtaining mutants with very high levels of constitutive activity.

Table 3: G_t Activation by Control Mutants and Double-Site Mutants in COS-Cell Membranes[a]

mutant	opsin[b] (%)	11-*cis*-retinal/dark[b] (%)	*all-trans*-retinal[b] (%)	11-*cis*-retinal/light[c] (%)
E113Q	23 ± 0.8	1.3 ± 0.5	111 ± 17	97 ± 18
E134Q	3.0 ± 1.2	1.2 ± 0.4	51 ± 26	98 ± 14
F261V[d]	7.6 ± 1.6	2.5 ± 0.4	43 ± 11	99 ± 14
E113Q/E134Q	31 ± 11	11 ± 8	98 ± 5	78 ± 6
E113Q/M257A	68 ± 8	18 ± 4	98 ± 11	73 ± 11
E113Q/M257N	74 ± 11	20 ± 3	133 ± 7	74 ± 6
E113Q/M257Y	81 ± 7	39 ± 9	83 ± 10	78 ± 14
E113Q/F261V	33 ± 4	4.5 ± 2.9	104 ± 8	78 ± 8
E134Q/M257A	47 ± 5	10 ± 3	106 ± 12	60 ± 3
E134Q/F261V	28 ± 2	1.9 ± 0.9	96 ± 10	69 ± 4

[a] Values indicate the ability of opsin alone, opsin with 11-*cis*-retinal in the dark, opsin with *all-trans*-retinal in the dark, and opsin with 11-*cis*-retinal in the light to activate G_t. Values are given as mean ± SE, $n = 3$ unless otherwise specified. [b] Opsin, 11-*cis*-retinal/dark, and *all-trans*-retinal activities are normalized to the 11-*cis*-retinal/light activity of the corresponding mutant measured in parallel. [c] Light activities in the presence of 11-*cis*-retinal are normalized to the light activity of wild-type opsin measured in parallel. [d] Data values from (*29*) and (*63*).

Mutations E113Q and E134Q in TM helix 3 cause relative constitutive activities of 23% and 3%, respectively (Table 3). Mutations M257A, M257N, M257Y, and F261V in TM helix 6 cause constitutive activities of 10%, 23%, 33%, and 8%, respectively (Tables 1 and 3). These mutants were combined to make the following double-site opsin mutants: E113Q/E134Q, E113Q/M257A, E113Q/M257N, E113Q/M257Y, E113Q/F261V, E134Q/M257A, and E134Q/F261V. A synergistic effect of a pair of mutations on constitutive activity can be evaluated by comparing the sum of the constitutive activities of two single-site mutant opsins with the experimental value of the double-site mutant. This comparison is demonstrated in a bar graph (Figure 4). The constitutive activities of the two single-site mutants and their sum are represented as stacked black and white bars. The constitutive activity of the corresponding double-site mutant is shown as a hatched bar. Any synergistic effect can be readily appreciated from the difference between the top of the stacked black and white bars and the top of the hatched bar.

These results demonstrate a synergistic effect of combining activating mutations in TM helix 3 with Met^{257} mutations. In some cases, this synergistic activation by double-site mutations is remarkably high. For example, three of the mutant opsins have constitutive activities that are close to their activities in light after reconstitution with 11-*cis*-retinal: E113Q/M257A (68%), E113Q/M257N (74%), and E113Q/M257Y (81%) (Table 3). They all consist of the counterion mutation E113Q in TM helix 3 and an activating Met^{257} mutation in TM helix 6. There is only a small synergistic effect when both activating mutations occur in TM helix 3 in mutant E113Q/E134Q. The mutant opsin E134Q/F261V also displays synergistic constitutive activity, while the mutant opsin E113Q/F261V does not (Table 3).

DISCUSSION

The Role of Met^{257} in Rho Function. The results described above show that Met^{257} in TM helix 6 of Rho is not critical for proper receptor folding, nor does it participate directly

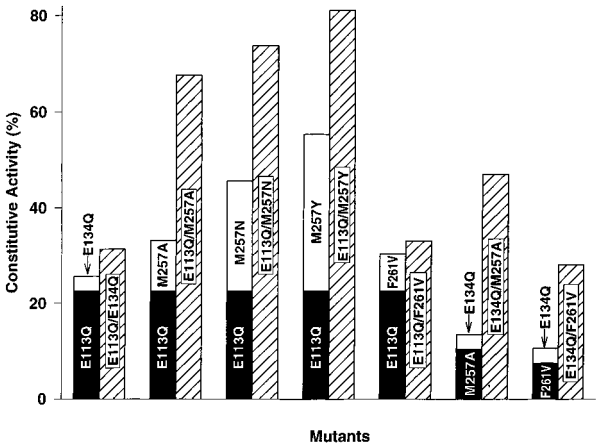

FIGURE 4: Replacement of both Met[257] and a residue in TM helix 3 produces opsin mutants with high levels of constitutive activity. The bar graph shows the levels of constitutive activity for five opsins with single-site mutations and seven opsins with double-site mutations. The opsin mutants are grouped in sets of three so that the effects of single mutations can be compared to the effects of double mutations. Black bars and white bars show the constitutive activity levels of opsin mutants with single-site replacements. The bars are stacked so that the sum of the activities of the two single-site mutants can be compared to the activity of the corresponding double-site mutant. Hatched bars represent the constitutive activity levels of opsin mutants with double-site replacements. The difference between the hatched bars and the sum of the stacked black and white bars represents a synergistic effect of the double mutation on the level of constitutive activity. For example, the constitutive activity of opsin mutant E134Q/M257A is much higher than the sum of constitutive activities of opsin mutants M257A and E134Q. Significant synergistic effects are noted when simultaneous mutations of Met[257] and a residue in TM helix 3 are introduced. Numerical values for the double mutants are summarized in Table 3.

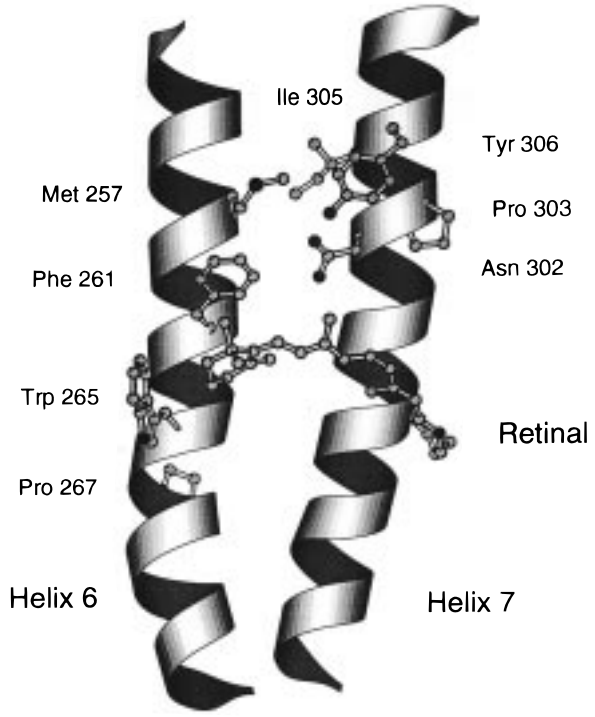

FIGURE 5: Molecular graphics model of Rho. TM helices 6 and 7 of Rho are viewed from the interior of the protein. The retinal chromophore is covalently atttached to Lys[296] on TM helix 7 with its cyclohexenyl ring packed between Phe[261] and Trp[265] on TM helix 6. Met[257] is one helical turn toward the cytoplasmic surface from Phe[261] and is predicted to pack among a cluster of residues: Asn[302], Ile[305], and Tyr[306]. The sequence motif NPXXY, corresponding to Asn[302]-Pro[303]-Val[304]-Ile[305]-Tyr[306] in Rho, is conserved in the GPCR family and may be involved in receptor activation.

in defining the ligand-binding site. However, mutagenesis of Met[257] has a dramatic effect on the basal activity of the resulting mutant opsin. Any amino acid replacement at position 257 other than leucine results in a receptor with elevated basal activity in the absence of retinal chromophore (Figure 2). Thus, Met[257] can be included with other sites in Rho where certain amino acid substitutions result in constitutive activity: Asp[90], Glu[113], Glu[134], and Lys[296] (*15*). The relative constitutive activities of the 17 mutant opsins with substitutions of Met[257] ranged from 2.6% to 32.6%, compared to the 0.9% relative basal activity of wild-type opsin assayed under the same conditions (Table 1).

There is no readily discernible correlation between the level of constitutive activity and any chemical property of the amino acid side chain at position 257. This is similar to the case observed with mutagenesis of Ala[293] in the α_{1B}-adrenergic receptor (*39*). Ala[293] is located near the N-terminus of TM helix 6, equivalent to the position of Thr[251] in Rho (Figure 1). These findings are in contrast to a complete mutagenesis study of Asp[142] located at the C-terminus of TM helix 3 of the α_{1B}-adrenergic receptor, equivalent to the position of Glu[134] in Rho (Figure 1), where the level of constitutive activation was best correlated with the hydropathy index of the amino acids evaluated (*40*). In addition, a careful study of activating mutations of Rho at positions Glu[134] and Lys[296] found that neutralizing the charge at position 134 and increasing the size at position 296 correlated positively with constitutive activity (*41*). Neutralizing the charge at position Glu[134] was consistent with the hypothesized role of Glu[134] in proton uptake in forming the active MII state of Rho (*42*, *43*).

Possible Interactions between Met[257] and the Conserved NPXXY Motif in TM Helix 7. The lack of strong correlation between the level of constitutive activity and any single physicochemical property of the entire set of amino acid side chains tested at position 257 suggests that Met[257] may be involved in a precise intramolecular interaction that can be disrupted by nearly any mutation. Side chain volume is correlated with opsin activity, but only for a subset of the replacements tested. In this context, it is interesting that mutant opsin M257L, the most conservative amino acid substitution possible, displays a wild-type phenotype for nearly all properties tested.

One of the most highly conserved sequence motifs in GPCR's is NPXXY near the cytoplasmic surface of TM helix 7 (*48*). Although the third and fourth positions of the pentapeptide are not conserved, they always consist of large hydrophobic residues such as valine, leucine, isoleucine, or phenylalanine (*48*). In bovine Rho, the conserved pentapeptide corresponds to Asn[302], Pro[303], Val[304], Ile[305], and Tyr[306]. Molecular graphics models of Rho, based on high-resolution cryoelectron microscopy and sequence homology (*44*−*46*) (Figure 5), show that the Met[257] side chain is situated in the interface between TM helices 6 and 7, and is tightly packed among side chains of Asn[302], Ile[305], and Tyr[306] in TM helix 7. The close proximity of TM helices 6 and 7 near their cytoplasmic borders can also be appreciated in the recent projection structure of frog Rho (*49*). Any substitutions other

than leucine may be expected to disrupt the interface between TM helix 6 and the NPXXY motif in TM helix 7. This in turn would allow flexibility or movement in the TM helical bundle to cause constitutive activation of the receptor. Helix movement has already been implicated in the molecular mechanism of Rho photoactivation (*47*).

Interactions between TM Helices 3 and 6 in Receptor Function. A series of elegant studies using site-directed mutagenesis of Rho in combination with spin-labeling and EPR spectroscopy has revealed that the molecular mechanism of receptor activation after chromophore isomerization involves outward rigid-body movements of TM helices 3 and 6 relative to the center of the helix bundle (*47*, *50*, *51*). Cross-linking of these helices near the cytoplasmic surface of the receptor by engineered disulfide bonds (*47*), or by chelated metal ions (*52*), prevents receptor activation. It is reasonable to assume that such a molecular mechanism for receptor activation may apply to constitutive activation as well. In this context, it is interesting to note that the majority of activating mutations reported in GPCR's are found in TM helix 6 (Figure 1), the same helix that contains Met^{257}. Furthermore, Cohen et al. (*53*) showed for Rho that disruption of a salt bridge between Glu^{113} in TM helix 3 and Lys^{296} in TM helix 7 by neutralization of either residue by mutagenesis leads to increased opsin activity. These findings imply that decreasing interhelical stabilizing interactions may lead to constitutive activity.

In apo-receptors with low basal activities, helix movements are prevented by stabilized helix−helix interaction that can be further enhanced by the binding of an inverse agonist ligand. Activating mutations may cause protein structural changes that shift the equilibrium between the inactive and the active conformations of the receptor. It is also possible that some mutations cause cytoplasmic interhelical loops to adopt a conformation similar to that of the active state by disrupting helix−helix interactions. According to some induced-fit models of receptor−G protein interaction, this might be expected to allow G protein binding to further stabilize the receptor active state (*54*). It is not surprising that the cytoplasmic border of TM helix 6 is one of the hot spots for activating mutations given the important role for this cytoplasmic region in G protein coupling (*55*, *56*).

A synergistic effect on constitutive activity was noted when separate mutations were introduced on each of the TM helices 3 and 6. The level of constitutive activity in several double-site mutants was significantly higher than the sum of the activities of each of the single-site mutants (Figure 4, Table 3). Numerous studies have shown that both the cytoplasmic loops linking TM helices 3 to 4 and helices 5 to 6 are directly involved in G_t binding and activation (*55*, *57*). Movements of TM helices 3 and 6, as revealed by site-directed spin-labeling studies, are likely to cause conformational changes in the connecting loops (*47*). Interestingly, it has also been shown that peptides corresponding to part of the 3−4 and 5−6 loops can synergistically compete with R* for G_t binding (*54*). This finding implies that the conformational changes in both loops concomitant with receptor activation may function cooperatively to bind and activate G_t. Activating single-site mutations in TM helices 3 or 6, for example, at Glu^{113} or Met^{257}, respectively, may switch only some of the receptor determinants of the active state from "off" to "on" as has been previously hypothesized (*58*). Changes in any of these determinants can shift the equilibrium between the active and inactive states of the receptor. According to this model of receptor activation, activating mutations in TM helices 3 and 6 could act synergistically to give very high levels of constitutive activity if combined. This is the case observed for opsin mutants E113Q/M257A, N, and Y, which display levels of constitutive activity as high as 80% of the level of light activation. The highest level of constitutive activity that we measured for any single-site mutant was 33% for mutant M257Y. A similar synergistic effect was observed in the α_1-adrenergic receptor for mutations in TM helices 3 and 5 (*59*).

Effects of Introducing Proline Residues in TM Helix 6 in GPCR's. The opsin mutant M257P is severely impaired in light-induced G_t activation after 11-*cis*-retinal regeneration as measured both in COS-cell membranes and in DM. In some other GPCR's, substitution of TM helix 6 residues by proline has been found to cause loss of function. For example, the D578P mutant of the LH receptor, corresponding to Phe^{261} in Rho, displays neither agonist binding nor effector response, possibly due to lack of receptor expression in the cell membranes (*8*). The G273P mutant of the neurokinin 2 receptor, corresponding to Ile^{275} in Rho, can bind antagonist, but not neurokinin A peptide (*60*). The A593P mutant of the LH receptor, corresponding to Phe^{276} in Rho, causes male pseudohermaphroditism. The mutant receptor can bind choriogonadotropin with normal affinity but fails to increase cAMP production (*61*). These positions, where the introduction of a proline disrupts the structure or function of the receptor, are shown in Figure 1 as diamonds.

The Relationship between Constitutive Activity and all-trans-Retinal Binding by Mutant Opsins Supports the Two-State Model of GPCR Function. The *all-trans*-retinal chromophore, when converted from 11-*cis*-retinal by photon absorption in the ligand-binding site, is the natural agonist of Rho. The activation of G_t by Rho under these conditions can be defined as 100%. However, when added exogenously to membranes containing opsin, *all-trans*-retinal only activates the apo-receptor to 14% of the light-induced activity of Rho. In this context, *all-trans*-retinal functions as a partial agonist in opsin. This observation is not surprising given that the physiologic function of Rho is to detect photons rather than *all-trans*-retinal. Opsin binds 11-*cis*-retinal preferentially over *all-trans*-retinal, and *all-trans*-retinal does not compete for 11-*cis*-retinal incorporation (*62*). The ligand preference for different retinal isomers can be altered by mutagenesis of residues in the retinal-binding site. We reported previously that the opsin mutant G121L binds *all-trans*-retinal preferentially over the 11-cis isomer and that mutant opsins with substitutions of Gly^{121} have significantly elevated activity in the presence of *all-trans*-retinal (*35*). Furthermore, opsin mutant M257A was shown to be fully activated by *all-trans*-retinal in COS-cell membranes and to form a covalent bond with the ligand that was stable enough to be purified in DM (*29*). In opsin mutant M257A, exogenously added *all-trans*-retinal can function as a full agonist.

In this study, we measured the ability of each of the Met^{257} mutant opsins to activate G_t in the presence of *all-trans*-retinal in membranes. There is a striking correlation between basal opsin activity and activity in the presence of *all-trans*-

retinal (ATR activity) as shown in Figure 3. For the set of 19 opsins tested, relative ATR activity increases rapidly as the relative basal opsin activity increases. A plateau in relative ATR activity of nearly 100% is reached when the relative basal activity is above about 10%. The relationship between constitutive activity and agonist ligand binding and activation can be described by the two-state model of GPCR function first proposed by Lefkowitz and co-workers (*31*).

The results presented in Figure 3 are a quantitative experimental test of the two-state model of GPCR function as described quantitatively by Jeff (*30*). Namely, the equilibrium constant L (L = [R]/[R*], where [R] and [R*] are the concentrations of apo-receptor in the inactive and the active states, respectively) is related to the level of basal opsin activity listed in Table 1 by the formula: 1/(opsin activity) − 1. We showed previously that at the concentration of *all-trans*-retinal (167 μM) used to assay ATR activity, opsin is fully saturated with the ligand (*35*). The ATR activity observed then reflects the maximum fraction of receptor in the active form (f_{R^*}). The two-state model predicts that the maximum partition of the active receptor is related to the equilibrium constant L by the formula $f_{R^*} = 1/(1 + LK_{A^*}/K_A)$, where K_{A^*} and K_A are the equilibrium constants of receptor bound to ligand A in its active and inactive states (K_{A^*} = [R*][A]/[AR*], K_A = [R][A]/[AR]) (*30*). The two-state model predicts that the increased basal activity (i.e., a decrease in L) will result in increased ATR activity (maximum f_{R^*}), which would eventually reach a saturation level of 1 when L is sufficiently small. If a constant $k = K_{A^*}/K_A$ is assumed for all of the mutants, then the correlation between ATR activity and opsin basal activity can be described by the function: ATR activity = (opsin activity)/[(1 − k)(opsin activity) + k], which is plotted as a curve in Figure 3. Most of the mutants follow the ideal curve very well with a k of 0.027 and a standard error of 16%. A k value of 0.027 for *all-trans*-retinal means that the ligand has ∼37-fold higher affinity for the active form of the receptor than the inactive form.

We have characterized in detail over 30 Rho mutants in addition to the Met^{257} mutant opsins reported here (*29*, *35*). Together, they comprise 50 mutant opsins with substitutions at 8 different sites in TM helices 3, 5, and 6. These mutants display a wide spectrum of biochemical phenotypes. However, the relationship between basal opsin activity and activity in the presence of *all-trans*-retinal (ATR activity) shown in Figure 3 holds for the entire set of 50 mutants. The correlation is not specific for mutations only at Met^{257}. The results show that the relative ATR activity of the vast majority of Rho mutants increases rapidly as a function of relative constitutive activity. Once the basal activity is elevated to above about 10% due to mutation, *all-trans*-retinal becomes an agonist with full potency even when added exogenously. The entire set of Rho mutants follows the curve predicted by the two-state model very well, with a k of 0.026 and a standard error of 14%. This value is nearly identical to the value of 0.027 obtained with the Met^{257} mutants alone.

In summary, the two-state model of GPCR function fits the experimental data derived from Rho mutants with activating mutations of TM helices 3 and 6, including the 17 Met^{257} mutants newly described in this report. This is the first quantitative evidence that Rho follows the two-state model for receptor activation documented for GPCR's with diffusible ligands. This observation suggests that the proposed mechanism of Rho photoactivation involving movements of TM helices 3 and 6 (*47*, *52*) applies as well to some constitutively activating mutations. Helix 6 movement may be prevented in the inactive state by a specific interaction between Met^{257} and TM helix 7. The site of interaction between Met^{257} and TM helix 7 is likely to involve the highly conserved NPXXY sequence. Taken together, these results further strengthen the notion that the family of GPCR's shares a common molecular mechanism of receptor activation.

ACKNOWLEDGMENT

We thank Dr. Steve Lin for many helpful discussions, Dr. Rosalie Crouch and the NEI for the 11-*cis*-retinal, and Cliff Sonnenbrot for oligonucleotide synthesis.

REFERENCES

1. Cotecchia, S., Exum, S., Caron, M. G., and Lefkowitz, R. J. (1990) *Proc. Natl. Acad. Sci. U.S.A. 87*, 2896−2890.
2. Tiberi, M., and Caron, M. G. (1994) *J. Biol. Chem. 269*, 27925−27931.
3. Cohen, D. P., Thaw, C. N., Varma, A., Gershengorn, M. C., and Nussenzveig, D. R. (1997) *Endocrinology 138*, 1400−1405.
4. Bond, R. A., Leff, P., Johnson, T. D., Milano, C. A., Rockeman, H. A., McMinn, T. R., Apparsundaram, S., Hyek, M. F., Kenakin, T. P., Allen, L. F., and Lefkowitz, R. J. (1995) *Nature 374*, 272−276.
5. Burstein, E. S., Spalding, T. A., and Brann, M. R. (1997) *Mol. Pharmacol. 51*, 312−319.
6. Shenker, A., Laue, L., Kosugi, S., Merendino, J. J., Jr., Minegishi, T., and Cutler, G. B., Jr. (1993) *Nature 365*, 652−654.
7. Laue, L., Chan, W. Y., Hsueh, A. J. W., Kudo, M., Hsu, S. Y., Wu, S. M., Blomberg, L., and Cutler, G. B., Jr. (1995) *Proc. Natl. Acad. Sci. U.S.A. 92*, 1906−1910.
8. Kosugi, S., Mori, T., and Shenker, A. (1996) *J. Biol. Chem. 271*, 31813−31817.
9. Parma, J., Duprez, L., van Sande, J., Cochaux, P., Gervy, C., Mockel, J., Dumont, J., and Vassart, G. (1993) *Nature 365*, 649−651.
10. van Sande, J., Parma, J., Tonacchera, M., Swillens, S., Dumont, J., and Vassart, G. (1995) *J. Clin. Endocrinol. Metab. 80*, 2577−2585.
11. Parma, J., van Sande, J., Swillens, S., Tonacchera, M., Dumont, J., and Vassart, G. (1995) *Mol. Endocrinol. 9*, 725−733.
12. Pollak, M. R., Brown, E. M., Estep, H. L., McLaine, P. N., Kifor, O., Park, J., Hebert, S. C., Seidman, C. E., and Seidman, J. G. (1994) *Nat. Genet. 8*, 303−307.
13. Schipani, E., Kruse, K., and Jüppner, H. (1995) *Science 268*, 98−99.
14. Arvanitakis, L., Geras-Raaka, E., Varma, A., Gershengorn, M. C., and Cesarman, E. (1997) *Nature 385*, 347−350.
15. Rao, V. R., and Oprian, D. D. (1996) *Annu. Rev. Biophys. Biomol. Struct. 25*, 287−314.
16. Dryja, T. P., Berson, E. L., Rao, V. R., and Oprian, D. D. (1993) *Nat. Genet. 4*, 280−283.
17. Sieving, P. A., Richards, J. E., Naarendorp, F., Bingham, E. L., Scott, K., and Alpern, M. (1995) *Proc. Natl. Acad. Sci. U.S.A. 92*, 880−884.
18. Keen, T. J., Inglehearn, C. F., Lester, D. H., Bashir, R., Jay, M., Bird, A. C., and Jay, B. (1991) *Genomics 11*, 199−205.
19. Sullivan, J. M., Scott, K. M., Falls, H. F., Richards, J. E., and Sieving, P. A. (1993) *Invest. Ophthalmol. Visual Sci. 34*, 11494.
20. Rim, J., and Oprian, D. D. (1995) *Biochemistry 34*, 11938−11945.

21. Robinson, P. R., Cohen, G. B., Zhukovsky, E. A., and Oprian, D. D. (1992) *Neuron 9*, 719−725.
22. Rao, V. R., Cohen, G. B., and Oprian, D. D. (1994) *Nature 367*, 639−642.
23. Fahmy, K., Zvyaga, T. A., Sakmar, T. P., and Siebert, F. (1996) *Biochemistry 35*, 15065−15073.
24. Richard, E. A., and Lisman, J. E. (1992) *Nature 356*, 336−338.
25. Li, T., Franson, W. K., Gordon, J. W., Berson, E. L., and Dryja, T. P. (1995) *Proc. Natl. Acad. Sci. U.S.A. 92*, 3551−3555.
26. van Rhee, A. M., and Jacobson, K. A. (1996) *Drug Dev. Res. 37*, 1−38.
27. Porcellini, A., Ciullo, I., Laviola, L., Amabile, G., Fenzi, G., and Avvedimento, V. E. (1994) *J. Clin. Endocrinol. Metab. 79*, 657−661.
28. Kosugi, S., and Mori, T. (1996) *Biochem. Biophys. Res. Commun. 222*, 713−717.
29. Han, M., Lin, S. W., Minkova, M., Smith, S. O., and Sakmar, T. P. (1996) *J. Biol. Chem. 271*, 32337−32342.
30. Leff, P. (1995) *Trends Pharmacol. Sci. 16*, 89−97.
31. Lefkowitz, R. J., Cotecchia, S., Samama, P., and Costa, T. (1993) *Trends Pharmacol. Sci. 14*, 303−307.
32. Lo, K., Jones, S. S., Hackett, N. R., and Khorana, H. G. (1984) *Proc. Natl. Acad. Sci. U.S.A. 81*, 2285−2289.
33. Ferretti, L., Karnik, S. S., Khorana, H. G., Nassal, M., and Oprian, D. D. (1986) *Proc. Natl. Acad. Sci. U.S.A. 83*, 599−603.
34. Franke, R. R., Sakmar, T. P., Oprian, D. D., and Khorana, H. G. (1988) *J. Biol. Chem. 263*, 2119−2122.
35. Han, M., Lin, S. W., Smith, S. O., and Sakmar, T. P. (1996) *J. Biol. Chem. 271*, 32330−32336.
36. Kaushal, S., and Khorana, H. G. (1994) *Biochemistry 33*, 6121−6128.
37. Wimley, W. C., and White, S. H. (1996) *Nat. Struct. Biol. 3*, 842−848.
38. Chothia, C. (1975) *Nature 254*, 304−311.
39. Kjelsberg, M. A., Cotecchia, S., Ostrowski, J., Caron, M. G., and Lefkowitz, R. J. (1992) *J. Biol. Chem. 267*, 1430−1433.
40. Scheer, A., Fanelli, F., Costa, T., de Benedetti, P. G., and Cotecchia, S. (1997) *Proc. Natl. Acad. Sci. U.S.A. 94*, 808−813.
41. Cohen, G. B., Yang, T., Robinson, P. R., and Oprian, D. D. (1993) *Biochemistry 32*, 6222−6115.
42. Fahmy, K., and Sakmar, T. P. (1993) *Biochemistry 32*, 7229−7236.
43. Arnis, S., Fahmy, K., Hofmann, K. P., and Sakmar, T. P. (1994) *J. Biol. Chem. 269*, 23879−23881.
44. Schertler, G. F. X., Villa, C., and Henderson, R. (1993) *Nature 362*, 770−772.
45. Baldwin, J. M. (1993) *EMBO J. 12*, 1693−1703.
46. Shieh, T., Han, M., Sakmar, T. P., and Smith, S. O. (1997) *J. Mol. Biol. 269*, 373−384.
47. Farrens, D. L., Altenbach, C., Yang, K., Hubbell, W. L., and Khorana, H. G. (1996) *Science 274*, 768−770.
48. Probst, W. C., Snyder, L. A., Schuster, D. I., Brosius, J., and Sealfon, S. C. (1992) *DNA Cell Biol. 11*, 1−20.
49. Unger, V. M., Hargrave, P. A., Baldwin, J. M., and Schertler, G. F. X. (1997) *Nature 389*, 203−206.
50. Farahbakhsh, Z. T., Ridge, K. D., Khorana, H. G., and Hubbell, W. L. (1995) *Biochemistry 34*, 8812−8819.
51. Altenbach, C., Yang, K., Farrens, D. L., Farahbakhsh, Z. T., Khorana, H. G., and Hubbell, W. L. (1996) *Biochemistry 35*, 12470−12478.
52. Sheikh, S., Zvyaga, T. A., Lichtarge, O., Sakmar, T. P., and Bourne, H. R. (1996) *Nature 383*, 347−350.
53. Cohen, G. B., Oprian, D. D., Yang, T., and Robinson, P. R. (1992) *Biochemistry 31*, 12592−12601.
54. König, B., Arendt, A., McDowell, J. H., Kahlert, M., Hargrave, P. A., and Hofmann, K. P. (1989) *Proc. Natl. Acad. Sci. U.S.A. 86*, 6878−6882.
55. Franke, R. R., Sakmar, T. P., Graham, R. M., and Khorana, H. G. (1992) *J. Biol. Chem. 267*, 14767−14774.
56. Strader, C. D., Fong, T. M., Tota, M. R., and Underwood, D. (1994) *Annu. Rev. Biochem. 63*, 101−132.
57. Franke, R. R., König, B., Sakmar, T. P., Khorana, H. G., and Hofmann, K. P. (1990) *Science 250*, 122−125.
58. Fahmy, K., Siebert, F., and Sakmar, T. P. (1995) *Biophys. Chem. 56*, 171−181.
59. Hwa, J., Gaivin, R., Porter, J. E., and Perez, D. M. (1997) *Biochemistry 36*, 633−639.
60. Bhogal, N., Donnelly, D., and Findlay, J. B. (1994) *J. Biol. Chem. 269*, 27269−27274.
61. Kremer, H., Kraaij, R., Toledo, S. P. A., Post, M., Friedman, J. B., Hayashida, C. Y., van Reen, M., Milgrom, E., Ropers, H., Mariman, E., Themmen, A. P. N., and Brunner, H. G. (1995) *Nat. Genet. 9*, 160−164.
62. Jäger, S., Palczewski, K., and Hofmann, K. P. (1996) *Biochemistry 35*, 2901−2908.
63. Han, M., Lou, J., Nakanishi, K., Sakmar, T. P., and Smith, S. O. (1997) *J. Biol. Chem. 272*, 23081−23085.
64. Ren, Q., Kurose, H., Lefkowitz, R. J., and Cotecchia, S. (1993) *J. Biol. Chem. 268*, 16483−16487.
65. Kremer, H., Mariman, E., Otten, B. J., Mol, G. W., Jr., Stoelinga, G. B. A., Wit, J. M., Jansen, M., Drop, S. L., Faas, B., Ropers, H.-H., and Brunner, H. G. (1993) *Hum. Mol. Genet. 2*, 1779−1783.
66. Yano, K., Saji, M., Hidaka, A., Moriya, N., Okuno, A., Kohn, L. D., and Cutler, G. B., Jr. (1995) *J. Clin. Endocrinol. Metab. 80*, 1162−1168.
67. Konopka, J. B., Margarit, S. M., and Dube, P. (1996) *Proc. Natl. Acad. Sci. U.S.A. 93*, 6764−6769.
68. Sung, C.-H., Davenport, C. M., and Nathans, J. (1993) *J. Biol. Chem. 268*, 26645−26649.

BI980147R